Research Article

Direct conversion of methane to C_2 hydrocarbons using W supported on sulfated zirconia solid acid catalyst

Md Ashraful Abedin[1] · **Srikar Bhattar**[1] · **James J. Spivey**[1]

Received: 17 August 2020 / Accepted: 26 October 2020 / Published online: 18 November 2020

Abstract
One of the most challenging aspects of modern day catalysis is the activation of methane. Conventionally, methane is activated with oxidizing agents to produce syngas, which then reacts to produce high value hydrocarbons. This process is energy inefficient. A more economic process is the direct one-step activation of methane to form value-added chemicals. This report focuses on direct conversion of methane to ethylene and ethane. Ethylene and ethane are the most important feedstocks in modern day chemical industries. Conventional process for ethylene production is via steam cracking of hydrocarbons, which is not an energy efficient approach. A direct conversion route from methane to C_2 hydrocarbons would be a significant advance and has been widely studied. Mo supported on solid acids have been previously reported to be promising for direct conversion of methane to higher hydrocarbons. Here, a novel catalytic approach is introduced with W, a strong oxidizing agent, doped on sulfated zirconia solid acid and studied for the activation of methane at 650–750 °C. BET, DRIFTS, ammonia TPD, XPS, XRD and SEM–EDX were used to characterize the fresh catalyst. Reaction products are primarily ethylene and ethane, along with trace aromatics. Methane activation along with production of C_2 hydrocarbons increased noticeably at higher temperature but deactivated due to carbon deposition as confirmed by TPO.

Keywords Methane activation · Tungsten oxide · Sulfated zirconia · Ethylene · Solid acid

1 Introduction

The growing need for heavier hydrocarbons in chemical industries has reached a new height in the twenty-first century. Over the last few decades, extensive research has been carried out to directly convert methane, the major component of natural gas, to value-added chemicals using heterogeneous catalysts [1]. An increased production of natural gas has led to a reduction in natural gas price compared to crude oil. Currently, the major use of natural gas is power generation and heating [2]. Despite extensive research for alternative uses, much of the natural gas produced as by-products of oil recovery is combusted and released [3], which is not an economic and environment friendly utilization of this major natural resource. Current industrial technologies for the conversion of natural gas are indirect processes, which are based on energy inefficient and involve complex steps involving the production of syngas (CO and H_2) [4]. Direct conversion routes can eliminate the requirement of this intermediate step [5, 6] and produce valuable chemicals with high energy efficiency.

Conventional processes of producing ethane and ethylene from methane involves the presence of oxidant, i.e., O_2, CO_2, S. One indirect approach is known as oxidative coupling of methane (OCM) [7]. Reported in early 1980s by Bhasin and Keller [8] as well as Hinsen and Baerns [9], this mechanism involves extraction of a hydrogen atom from

Electronic supplementary material The online version of this article (https://doi.org/10.1007/s42452-020-03761-4) contains supplementary material, which is available to authorized users.

✉ James J. Spivey, jjspivey@lsu.edu | [1]Cain Department of Chemical Engineering, Louisiana State University, Baton Rouge, LA, USA.

methane to activate it and produce methyl intermediates. This methyl radical may react with another one to produce ethane. If another hydrogen atom can be extracted from the methyl radical, it would generate CH_2* intermediate, which may react with a similar radical to produce ethylene. Studies have shown that mixed metal oxides like La-based perovskites [10], MnNaW/SiO_2 [11], Mo/HZSM-5 [12, 13] and noble metals [14] help oxidize methane toward ethylene and ethane. The challenge of this approach is that selectivity to C_2s has been reported to be relatively low and the process involves high temperature with complex intermediates [5] which make the whole process less efficient.

A similar mechanism can also be proposed for direct activation of methane to C_2 hydrocarbons. Progress has been made toward understanding how methane can be directly activated by forming methyl radicals [15], without the involvement of coreactants, which may further react to produce higher hydrocarbons. This route of methane activation to ethane and ethylene requires the presence of a solid acid catalyst [16]. The reaction has two important pathways, one converts methane to ethane and the other produces ethylene (Fig. 1).

Thermodynamically, such methane activation pathways ultimately drive the reaction spontaneously toward formation of solid carbon [1, 17], which is the most stable product at equilibrium conditions. In order to drive the selectivity toward C_2s, an oxide heterogeneous catalyst is necessary [18–20].

One of the most important properties needed for such catalysts is the ability to form oxygen vacancies [21]. For strong oxidizing agents, oxygen vacancies are readily formed. This is the similar mechanism that enables methane during OCM to convert and selectively produce C_2 hydrocarbons. A recent DFT study by Cheng et al. [22] suggested that a limited increase in concentration of oxygen vacancy on the oxide-based catalyst results in significant decrease in the energy required for the hydrogen extraction to break the methane molecule and form methyl radicals. Oxygen vacancies thus can promote the direct conversion of methane.

Here, this study focuses on using W oxide-based acid catalyst. Previously, transition metals of group VIB have shown activity for alkane activation [23, 24]. Mo/W oxide supported on ZSM-5/MCM-22 is a well-studied bifunctional catalyst for methane dehydroaromatization [2, 25]. It has been reported that the metal carbide species produced from Mo/W oxides activate methane by forming CH_x species, which is dimerized into C_2H_y species [13, 26]. Previously, this group demonstrated high activity and strong aromatic selectivity for methane dehydroaromatization (MDHA) using Mo oxide doped on sulfated zirconia (SZ) solid acid catalysts [15]. During these studies, it was observed that the addition of W as promoter to Mo/SZ shifted the MDHA product selectivity toward ethylene and ethane [24]. W is known to be a strong oxidizing agent [27, 28]. It reacts with rare earth elements, Fe, Cu, Al, Mn, Zn, Cr, Mo, C, H_2 and can be reduced to pure tungsten metal [29].

The rationale is to dope W oxide into a stable non-reducible oxide that exhibits high resistance to the loss of oxygen and low reactivity toward hydrogen at high temperature. Although silica and alumina have been reported as strong non-reducible catalyst supports [30, 31], recent studies have revealed zirconium oxides to demonstrate higher strength in working conditions [32]. It has been reported that the sulfurized form of ZrO_2 known as sulfated zirconia (SZ), actively helps the active metal sites to stabilize on the oxide support at a greater degree [29, 33]. SZ is a well-known solid acid possessing surface H + ions [29, 34], which can react with some of the excess methyl radicals and remove these in the form of benzene and heavier hydrocarbons as valuable side products [15, 35].

This present study is a follow-up of this group's recent works with sulfated zirconia-based solid acid catalysts for methane activation. Here, we introduce a novel catalytic approach, where W oxide is supported on SZ and investigate its effect on direct activation of methane. To the best of our knowledge, no study has shown methane activation with W/SZ catalyst to selectively produce C_2 hydrocarbons. Synthesis of this novel catalyst is followed by characterization using pyridine DRIFTS, BET, ammonia TPD, SEM–EDX, XPS, XRD and temperature programmed techniques. Afterward, W/SZ is tested to activate methane and its performance on C_2 product selectivity will be evaluated in thermodynamically favored reaction temperatures. This is followed by subsequent temperature programmed oxidative analysis on carbon deposition.

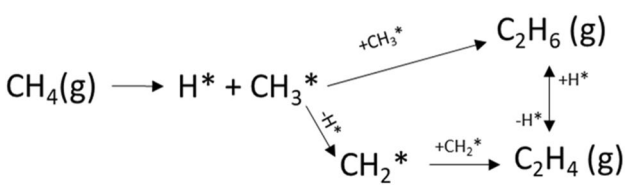

Fig. 1 Methane to C_2 hydrocarbons possible reaction pathways

2 Catalyst Preparation

2.1 Materials

Ammonium metatungstate hydrate, $(NH_4)6H_2W_{12}O_{40}{\cdot}xH_2O$ and zirconium hydroxide, $Zr(OH)_4$ (97%) precursors were purchased from Sigma-Aldrich Inc. H_2SO_4 (95–98.0%) was purchased from Malinckrodt Chemicals Inc. Ultrahigh

purity grade He, H_2, CH_4 and 10% O_2/He were ordered from Airgas Inc.

2.2 Synthesis

Sulfated zirconia was prepared by following conventional methods [24, 29]. 35 g of zirconium oxide was mixed with 500 mL of 0.5 M H_2SO_4 solution prepared with DI water. The mixture was stirred for 2 h, followed by vacuum filtration with excess DI water. The retentate was dried at 110 °C overnight followed by calcination at 550 °C for 4 h to prepare the final catalyst.

W/SZ was synthesized by following the preparation method of Mo/SZ [24, 32]. The catalyst was prepared using incipient wetness impregnation method with ammonium metatungstate hydrate as the precursor. W impregnation was carried out at room temperature. 5 wt% of W was added in the form of ammonium tungstate to 100 ml DI water mixture. 8 gm of prepared SZ was later added to this solution. The mixture was stirred for 2 h, followed by vacuum filtration with excess DI water. The sample was dried at 110 °C overnight and calcined at 550 °C in atmospheric condition for 4 h. The catalyst was passed through a sieve to achieve the final powdered form. Later, it was weighed and collected in glass ampule to avoid exposure to moisture and air.

3 Characterization Techniques

3.1 BET

Altamira AMI-200 characterization reactor was used for breauner emmett teller (BET) surface area measurement with N_2 monolayer adsorption. To measure the catalytic surface area, a three-point BET was used in the presence of 10%, 20% and 30% N_2 concentrations.

3.2 Ammonia TPD

Ammonia TPD was carried out in Altamira AMI-200 reactor system coupled with Ametek mass spectrometer. 50 mg of the prepared catalyst was loaded on a quartz U-tube reactor. Catalytic pretreatment was followed by using He as the inert gas source. Temperature was increased till 200 °C with 30 sccm of He flow and held for 30 min to eliminate any weakly physisorbed particles on catalytic surface. Sample temperature was cooled down to 50 °C under He, followed by introduction of 40 sccm of 5% NH_3/He to initiate NH_3 adsorption process for 90 min. 30 sccm He was flown subsequently for 40 min to get rid of any residual ammonia. Mass spec and TCD detector were later turned on, and the temperature was increased at 10 °C/min. from 50 to 700 °C. Based on the signal from mass spec and TCD, amounts of ammonia desorbed and peak positions were calculated to quantify the corresponding acid sites available on the catalyst.

3.3 Pyridine DRIFTS

Pyridine is a weak base and was used as a probe molecule for catalytic acid site characterization with diffuse reflectance infrared Fourier transform spectroscopy (DRIFTS). A Thermo Scientific Nicolet 6700 FTIR equipped with harrick praying mantis (HPM) reaction cell fitted with KBr windows was used for DRIFTS experiment.

Glovebox technique was used to load the HPM cell with catalyst powders to avoid atmospheric exposure. Helium was introduced in the cell initially to remove any residual moisture or physisorbed particles. This was followed by catalytic pretreatment by increasing the temperature to 100 °C and was held for 30–40 min to clean the surface from adsorbed impurities. To collect a background spectrum, sample temperature was reduced to 25 °C, and a spectral resolution of 4 cm^{-1} was recorded within the region of 2000–250 cm^{-1}. Gaseous pyridine was introduced to saturate the surface for 180 min at 25 °C. Helium was reintroduced in the follow-up step to remove the physisorbed pyridine at the catalyst surface and the IR cell walls. Temperature was raised at 100 °C again to desorb the pyridine that was bonded to the strong acid sites of the sample. It was held at 100 °C for 10 min and cooled back to room temperature to record the pyridine adsorption spectrum. Similar spectra were recorded at 25 °C after 10 min. This procedure was repeated at 200 °C, 300 °C and 400 °C to investigate thermal stability of the acid sites.

3.4 XPS

X-ray photoelectron spectroscopy was performed at Louisiana State University shared instrument facility (SIF) to understand the oxidation sates of the active metal. Samples were characterized using Scienta Omicron ESCA 2SR XPS instrument with aluminum monochromatic X-ray source at 15 kV with pass energy of 40. XPS data were analyzed using CasaXPS licensed software.

3.5 SEM–EDS

SEM–EDS analysis of the samples was performed to determine elemental composition at the bulk level. The experiment was carried out at LSU shared instrument facilities (SIF) using FEI quanta 3D FIB/SEM coupled with Ametek EDAX

accessory. Voltage of 5 kV and a resolution of 3 µm were maintained to detect elemental compositions.

3.6 XRD

PANanalytical EMPYREAN diffractometer with Cu K_α radiation was used to perform XRD analysis. Spectra were scanned between the 2 θ range of 5° to 90° with step size of 0.1°. XRD data were analyzed with licensed PANanalytical X'Pert software, and data comparison was done using MS Excel.

4 Experimental procedure

The prepared catalyst was run at a temperature range of 650–750 °C for ~ 15 h to investigate direct activation of methane. The catalysts were loaded in an Altamira AMI 200HP reactor system equipped with quartz tube reactor and reduced under H_2 flow till the desired reaction temperature was reached. This was followed by carburization while flowing a gas mixture of methane and H_2 (flow ratio 1:4), which was introduced into the reactor for 4 h to further reduce the catalyst. H_2 and CH_4 gases were stopped, and the reactor was purged with helium as inert gas. Methane was reintroduced later to carry out methane activation reaction.

Downstream reaction product gas was analyzed using Shimadzu GC2014 (FID, 2 TCDs) equipped with Restek RT-Q-bond column (30 m × 0.53 mm × 20 µm) in conjunction with Shimadzu QP2010 GC–MS system.

Conversion of methane was calculated with the following formula.

$$\%\ \mathrm{CH_4 conversion} = \frac{\mathrm{mol\ CH_{4\,in}} - \mathrm{mol\ CH_{4\,out}}}{\mathrm{mol\ CH_{4\,in}}} \times 100$$

Product selectivity was calculated based on the gaseous products observed from conversion of methane. Carbon deposition is excluded from this calculation as the coke formed at any instant of the reaction is not measured. Another reason for the exclusion is because the rate of coke formation differs over a period and is not discussed in this work.

$$\%\ \text{product selectivity} = \frac{\text{mol Product}}{\text{mol total products}} \times 100$$

5 Results and discussion

5.1 Physicochemical properties

BET physisorption showed that surface area of W/SZ was less than pure SZ (Table 1). Literature reports the surface area of SZ to be 50–100 m^2/g [36, 37]. When W was impregnated in SZ, a slight decrease in surface area indicates some blockage in porous regions of SZ due to loading of the active metal.

Table 1 Physico-chemical properties of W/SZ catalysts

Sample	W wt.% (intended)	W wt.% (SEM–EDS)	W wt.% (XPS)	BET surface area (m^2/g)
SZ	–	–	–	84
5% W/SZ	5	4.3	4.1	71

To determine the actual loading of W on SZ, SEM–EDS and XPS analysis were carried out. It was observed from both analysis that the actual amount of W was lower than the intended loading. This may be due to loss of W during catalytic synthesis.

5.2 Pyridine DRIFTS

Pyridine is typically used as a weak base to probe the strong acids sites of catalysts. DRIFTS analysis was carried out to investigate the stability of SZ acid sites, before and after W was loaded into the catalyst. Adsorbed pyridine sites on SZ correspond to either Brønsted, Lewis acid sites or dual acid sites, detected from the vibrational bands which can be distinguished between the types of acid sites.

Vibrations at around 1445 cm^{-1} and 1610 cm^{-1} represent Lewis acid sites, whereas vibrations at around 1545 cm^{-1} and 1645 cm^{-1} represent Brønsted acid sites [38]. Vibrations at around 1495 cm^{-1} represents sites that contain both Lewis and Brønsted acidity [38, 39]. All of these characteristic bands were observed in SZ catalysts, before and also after W loading (Fig. 2). This indicates that surface acidity was not compromised when active metals were impregnated into SZ. An increased intensity of Lewis acid sites on W/SZ refers to the addition of Lewis acidic W sites on SZ. The small peak at ~ 1580 cm^{-1} represents physisorbed pyridine [38].

Both catalysts were tested at temperatures up to 400 °C to study the stability of these acid sites at elevated temperatures. It was observed that both catalysts showed stable acid sites, as observed from Fig. 2.

5.3 Ammonia TPD

To quantify the amount of acidity in the catalysts before and after W addition, ammonia was used as a probe molecule for temperature programmed desorption (TPD). Ammonia is a weak base molecule with pK_b value of 4.5 [40].

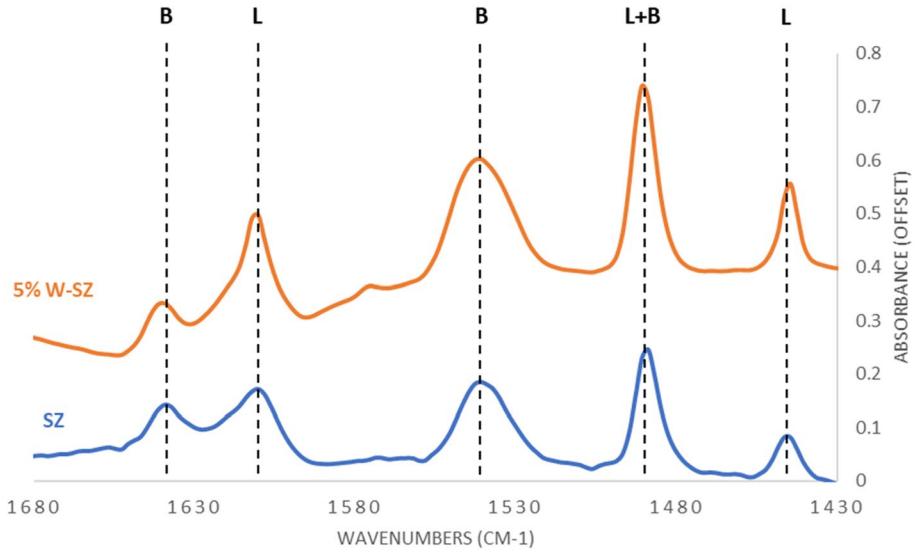

Fig. 2 DRIFTS of the prepared catalysts at 400 °C, after pyridine exposure for 3 h

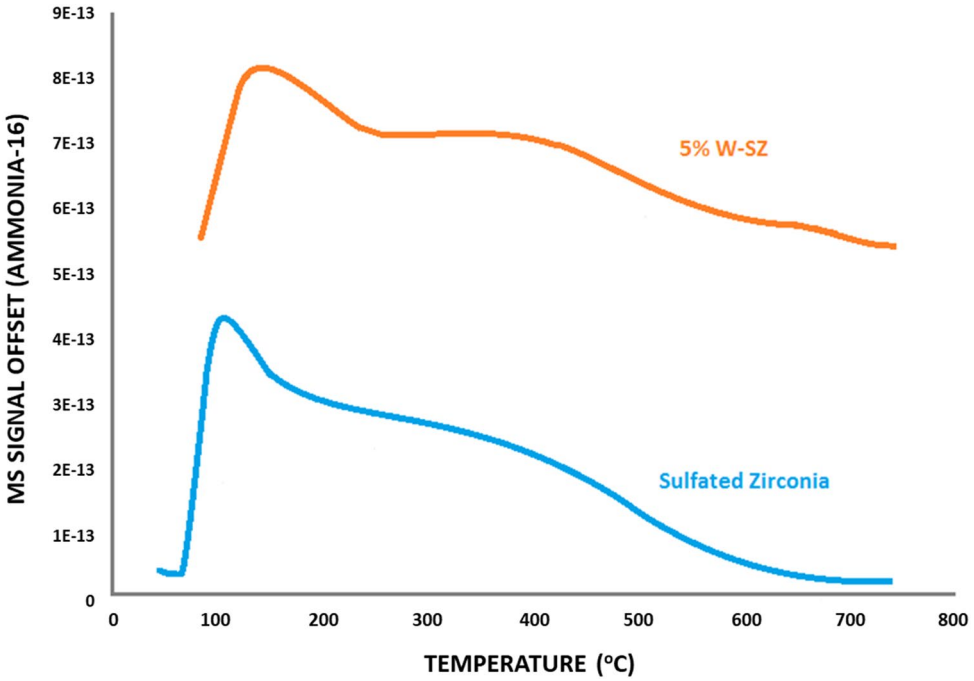

Fig. 3 NH_3-TPD of fresh catalysts, 40 sccm 5%NH_3/He flow, 50 mg

Figure 3 shows a comparison of ammonia TPD curves for the two catalysts: base SZ and W/SZ. SZ showed a typical ammonia TPD peak at ~ 120–140 °C range, followed by a long shoulder that drops down slowly to ~ 550 °C. W/SZ showed a very similar TPD curve as well, but the intensity in the TPD curve went down after loading W onto SZ, indicating an overall loss of the total acidity.

This decrease in total acidity with the addition of W to SZ was quantified by measuring the total TPD area for both SZ and W/SZ (Table 2). This can occur due to a possible blockage of microporous SZ channels by W oxide particles, thus restricting the access of ammonia to some acid sites.

Table 2 Amount of NH_3 desorbed/consumed per gram of catalyst

Catalyst	Total micromoles of NH_3 desorbed per gram catalyst
SZ	1953.6
5% W/SZ	1522.2

5.4 XRD

SZ has distinct XRD pattern widely reported in the literature [24, 32]. Different phases of SZ have been observed

based on the synthesis technique and calcination temperatures [37, 41]. In this work, since SZ was calcined at 550 °C. At this temperature tetragonal phases mostly dominate the chemical structure [29, 37]. Figure 4 shows the XRD spectra of SZ and W/SZ catalysts. Base SZ clearly showed all the characteristic peaks attributed to tetragonal phase (reference ICDD PDF # 811,544). After W was loaded onto SZ, no difference in XRD pattern is observed, suggesting that W is evenly dispersed into SZ structure in amorphous form, with little crystallinity. This also implies that base structure of SZ remained intact even after W was impregnated.

5.5 Activation of methane

The catalysts were tested for methane activation at different temperatures to understand their effect on activity and product selectivity. Before initiating the catalytic reaction, a blank reaction was carried out in the absence of the catalysts at reaction conditions. Only methane was observed in the product stream, detected by GC–MS. Afterward, three catalytic reactions were carried out for ~ 15 h each, at 650, 700 and 750 °C in otherwise identical reaction conditions. The products observed in all of the catalytic runs were primarily ethylene, ethane, with small amount of aromatics including BTEX (benzene, toluene, ethylbenzene and xylenes).

As expected, initial methane conversion increased with temperature, but quickly deactivated with time, reaching similar methane conversion with time at each temperature (Fig. 5). This can be attributed to catalytic deactivation due to carbon deposition. Even though methane conversion did not differ significantly with temperature after less than 100 min, product selectivity was significantly different.

Product selectivity toward C_2 hydrocarbons increased with temperature (Fig. 6). Selectivity increased initially for 650 °C and reached stability at ~ 70% after ~ 300 min of run. For 700 °C, selectivity dropped down initially and then reached a stable ~ 76% selectivity throughout the run. Highest amount of C_2 selectivity was observed for 750 °C, which went up initially for a short period of time and then became stable at ~ 93% throughout the run. This increase in C_2 selectivity with temperature can be attributed to more W active sites being reduced at a faster rate. When temperature increases, more W oxide are reduced [42], as a result more methyl radicals turn to C_2 dimers [24], thus produce ethylene and ethane.

Benzene was a major product observed at 650–700 °C, due to the enhanced acidity provided by SZ [15] (Fig. 7). For 650 °C, benzene selectivity was initially at ~ 35%, which decreased rapidly with time. A similar trend was also observed with 700 °C, where benzene selectivity increases initially and decreased rapidly with time as well. For 750 °C, very little benzene formation was observed, product selectivity was mostly C_2 hydrocarbons at this temperature. Acidity from SZ promoted methyl radicals to produce benzene instead of carbon. This transformation, however, was unstable in this case. Acidity of SZ is dependent on the available sulfate ions, which are responsible for supplying H^+ ions during the reaction. It has been reported that at temperatures higher than 630 °C, sulfate ions are not stable in dynamic reaction conditions [34], and leave SZ surface in gaseous states (SO_x). Thus, SZ loses the required acidity to transform methyl radicals to aromatics like benzene and is similar to ZrO_2, as observed from these runs.

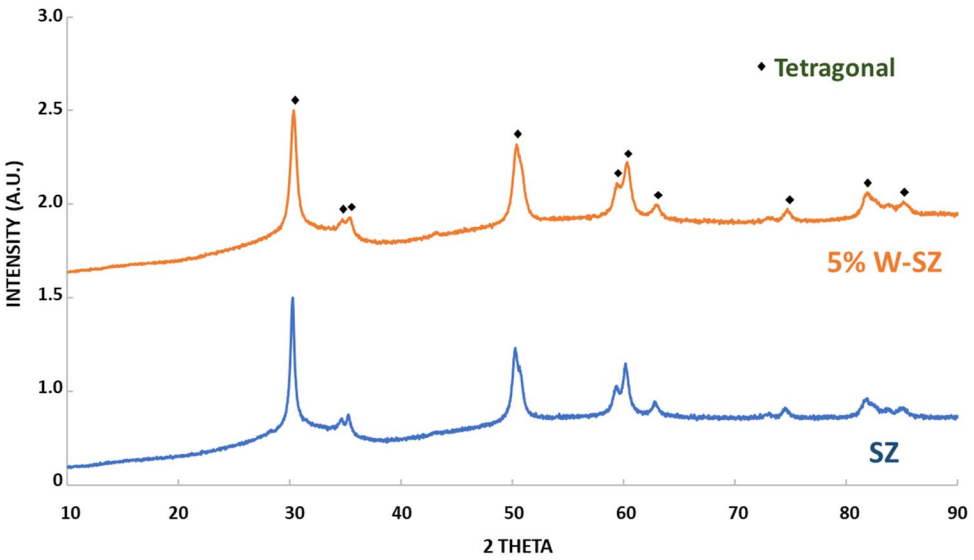

Fig. 4 XRD patterns of SZ and W/SZ

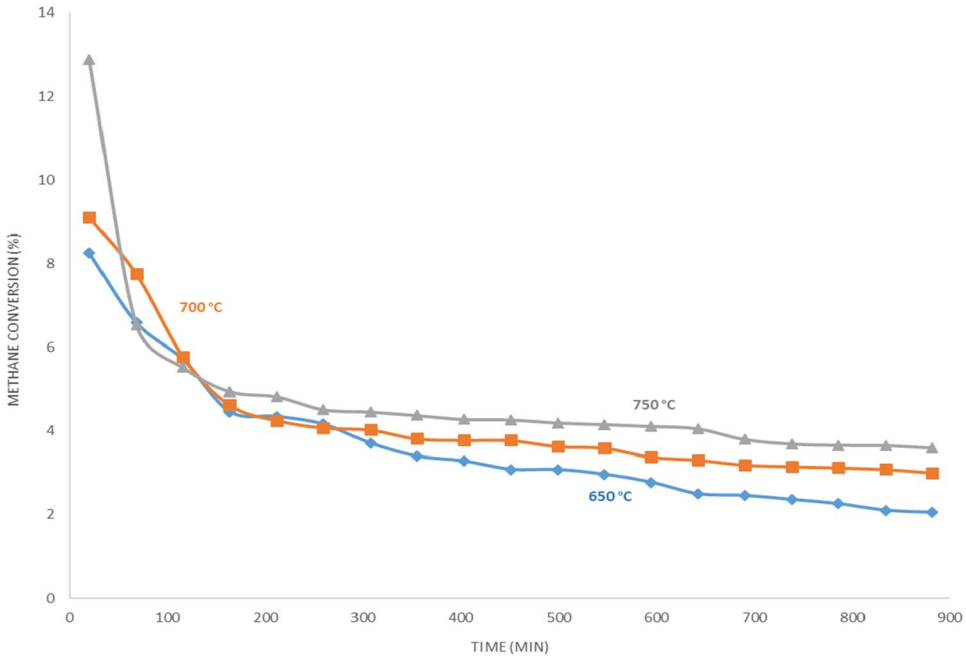

Fig. 5 Conversion of methane with 5% W/SZ, 1 g, 10 SCCM methane flow, 1 atm

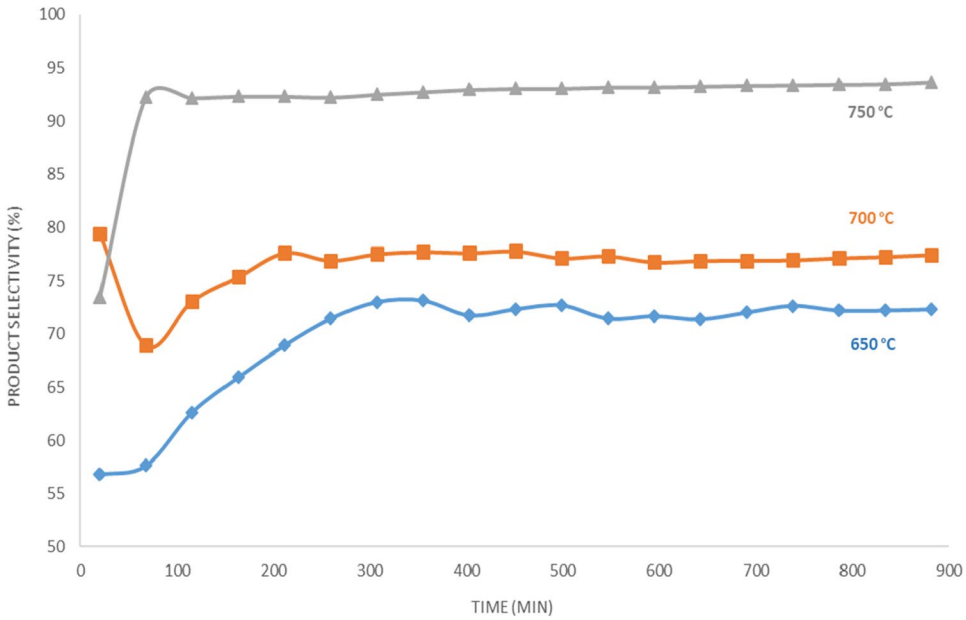

Fig. 6 C_2 product selectivity for methane conversion with 5% W/SZ, 1 g, 10 SCCM methane flow, 1 atm

5.6 Temperature programmed oxidation (TPO)

To understand the deactivation mechanism of W/SZ, TPO was carried out on each spent catalyst from the three temperature runs. Catalytic deactivation is mostly due to carbon deposition [43], which can be categorized as either amorphous, with a peak position at ~ 400 °C, or polymeric carbon generated from aromatics, with peak temperatures at 500–600 °C range, or graphitic carbon with peaks at 650–750 °C range [44].

Spent catalyst from 650 to 700 °C runs showed sharp TPO peaks at around 500–600 °C range, attributable to polymeric carbon (Fig. 8). Liu et al. [45]reported that Brønsted acid sites from SZ provide active sites for the formation of aromatics and lead to carbon formation as final product. At 650 °C, there was more aromatics formation than 700 °C, indicating that less sulfate ions are vaporized from the SZ surface at lower temperatures, thus producing more carbon precursors.

For the 750 °C spent catalyst, a small shoulder at 500–550 °C region indicates very little formation of

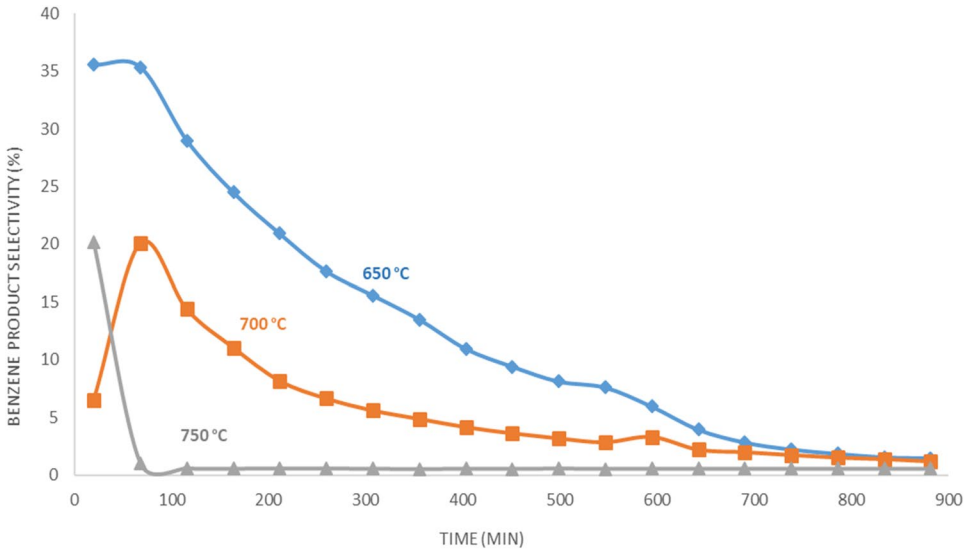

Fig. 7 Benzene product selectivity for methane conversion with 5% W/SZ, 1 g, 10 SCCM methane flow, 1 atm

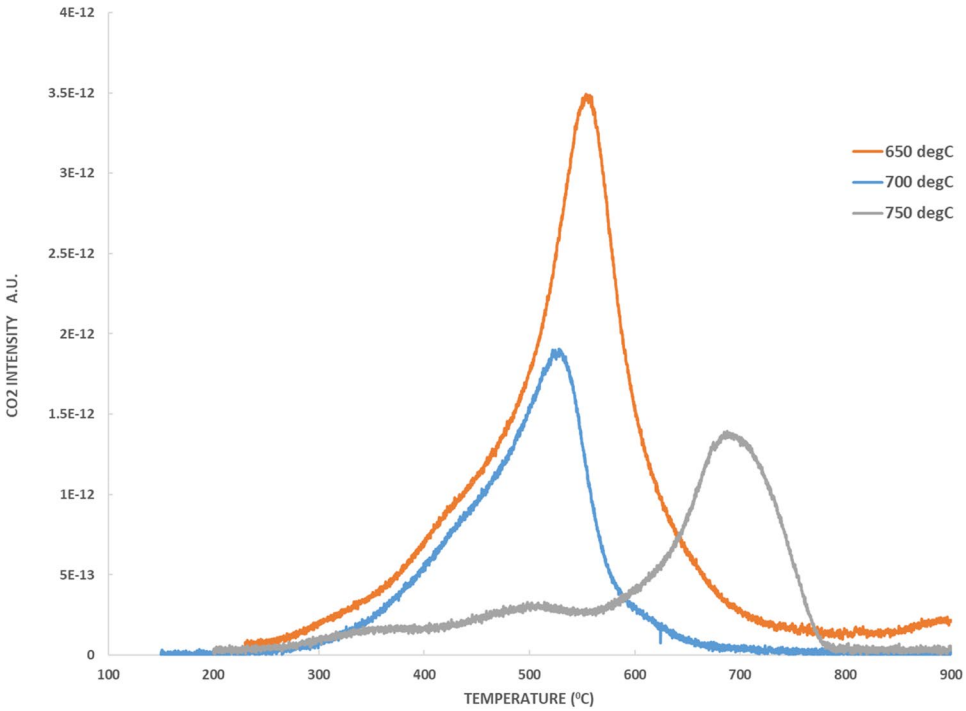

Fig. 8 TPO data for the three spent catalysts, 15 sccm O_2/He, 25 mg

polymeric carbon. A stronger peak at ~ 700 °C indicates the formation of graphitic carbon, which can be attributed to carbon from active metal or acid sites that are strongly attached to the catalytic surface [46]. This suggests that W oxides were greatly reduced at higher temperature to W carbides or oxycarbides, which are responsible for enhancing dehydrogenation activity [47–49], as observed during the 750 °C run.

Amount of carbon deposited was quantified for all three runs (Table 3). More carbon was observed from the 650 °C run with the highest aromatics formation, which is in accordance with the TPO analysis.

Table 3 Quantification for carbon deposition with TPO (after ~ 15 h of reaction)

W/SZ Catalysts (°C)	Carbon deposited (mmol/gcat)
650	5.94
700	3.27
750	3.11

6 Conclusion

Activation of methane was studied with novel W/SZ catalyst to study the correlation of the effect of reaction temperature with product selectivity. Previous studies with Mo/SZ successfully demonstrated high activity for MDHA, with affinity toward C_2 formation when W was present as a promoter [24]. The objective of this follow-up work was to use a similar novel approach to directly convert methane to C_2 hydrocarbons by introducing WO_x as the primary active site onto SZ solid acid, characterizing the catalyst and understanding the role of W toward C_2 hydrocarbons selectivity.

Characterization of SZ and W/SZ was carried out using pyridine DRIFTS and ammonia TPD, which confirmed that addition of W to SZ increased Lewis acid sites in SZ but decreased the total acidity. BET surface area measurements showed high dispersion of W active sites inside SZ pores. SEM–EDS and XPS confirmed that the actual loading of W was close to the intended amount. XRD suggested that W is well dispersed throughout SZ in amorphous form.

Experimental results showed that methane activation did not vary significantly with temperature, although change in product selectivity was observed. W/SZ was found to be highly selective to ethylene and ethane (~ 73–93% selectivity) at 650–750 °C, which was the primary goal of this study. C_2 selectivity increased with temperature and remained stable with time. Benzene was another major product observed at 650–700 °C range, which decreased rapidly with temperature and time due to possible loss of sulfate sites from SZ at high temperature. TPO results indicate that the primary reason of catalytic deactivation is due to polymeric(650–700 °C runs) and graphitic carbon deposition (750 °C run).

Acknowledgements Authors would like to acknowledge Dr. Dongmei Cao at Louisiana State Univeristy Shared Instrumentation Facility (LSU SIF) for helping with the X-Ray characterizations and Louisiana State University Office of Research and Economic Development (LSU ORED) for providing financial support throughout this work under program number PG-007981.

Funding Louisiana State University Office of Research and Economic Development (LSU ORED) under program number PG-007981.

Compliance with ethical standards

Conflict of interest The authors declare no conflict of interest.

References

1. Spivey JJ, Hutchings G (2014) Catalytic aromatization of methane. Chem Soc Rev 43(3):792–803. https://doi.org/10.1039/c3cs60259a
2. Karakaya C, Kee RJ (2016) Progress in the direct catalytic conversion of methane to fuels and chemicals. Prog Energy Combust Sci 55:60–97. https://doi.org/10.1016/j.pecs.2016.04.003
3. Adebajo M, Frost R (2012) Recent advances in catalytic/biocatalytic conversion of greenhouse methane and carbon dioxide to methanol and other oxygenates. In: Liu G (ed) Greenhouse: gases capturing utilization and reduction. InTech, Rijeka. https://doi.org/10.5772/32552
4. Chen H, Li L, Hu J (2017) Upgrading of stranded gas via non-oxidative conversion processes. Catal Today Ahead of Print. https://doi.org/10.1016/j.cattod.2017.05.029
5. Schwach P, Pan X, Bao X (2017) Direct conversion of methane to value-added chemicals over heterogeneous catalysts: challenges and prospects. Chem Rev 117(13):8497–8520. https://doi.org/10.1021/acs.chemrev.6b00715
6. Abedin MA, Kanitkar S, Bhattar S, Spivey JJ (2020a) Mo oxide supported on sulfated hafnia: novel solid acid catalyst for direct activation of ethane & propane. Appl Catal A 602:117696. https://doi.org/10.1016/j.apcata.2020.117696
7. Cai X, Hu YH (2019) Advances in catalytic conversion of methane and carbon dioxide to highly valuable products. Energy Sci Eng 7(1):4–29. https://doi.org/10.1002/ese3.278
8. Keller GE, Bhasin MM (1982) Synthesis of ethylene via oxidative coupling of methane: I. Determination of active catalysts. J Catal 73(1):9–19. https://doi.org/10.1016/0021-9517(82)90075-6
9. Papp H, Hinsen W, Do NT, Baerns M (1984) The adsorption of methane on H-ZSM-5 zeolite. Thermochim Acta 82(1):137–148. https://doi.org/10.1016/0040-6031(84)87282-2
10. Sim Y, Kwon D, An S, Ha J-M, Oh T-S, Jung JC (2020) Catalytic behavior of ABO3 perovskites in the oxidative coupling of methane. Mol Catal 489:110925. https://doi.org/10.1016/j.mcat.2020.110925
11. Uzunoglu C, Leba A, Yildirim R (2017) Oxidative coupling of methane over Mn-Na2WO4 catalyst supported by monolithic SiO2. Appl Catal A 547:22–29. https://doi.org/10.1016/j.apcata.2017.08.020
12. Matus E, Sukhova O, Ismagilov I, Zaikovskii V, Kerzhentsev M, Ismagilov Z, Dossumov K, Mustafin A (2009) Deactivation and regeneration of Mo/ZSM-5 catalysts for methane dehydroaromatization. Eurasian Chemico-Technol J. https://doi.org/10.18321/ectj19
13. Wan H, Chitta P (2016) Catalytic conversion of propane to BTX over Ga, Zn, Mo, and Re impregnated ZSM-5 catalysts. J Anal Appl Pyrol 121:369–375. https://doi.org/10.1016/j.jaap.2016.08.018
14. Wang L, Ohnishi R, Ichikawa M (1999) Novel rhenium-based catalysts for dehydrocondensation of methane with CO/CO2 towards ethylene and benzene. Catal Lett 62:29–33. https://doi.org/10.1023/a:1019022316715
15. Kanitkar S, Abedin MA, Bhattar S, Spivey JJ (2019) Methane dehydroaromatization over molybdenum supported on sulfated zirconia catalysts. Appl Catal A 575:25–37. https://doi.org/10.1016/j.apcata.2019.01.013
16. Guo X, Fang G, Li G, Ma H, Fan H, Yu L, Ma C, Wu X, Deng D, Wei M, Tan D, Si R, Zhang S, Li J, Sun L, Tang Z, Pan X, Bao X (2014) Direct, nonoxidative conversion of methane to ethylene, aromatics, and hydrogen. Science 344(6184):616–619. https://doi.org/10.1126/science.1253150
17. Bijani PM, Sohrabi M, Sahebdelfar S (2012) Thermodynamic analysis of nonoxidative dehydroaromatization of methane. Chem Eng Technol 35(10):1825–1832. https://doi.org/10.1002/ceat.201100436
18. Ismagilov ZR, Matus EV, Tsikoza LT (2008) Direct conversion of methane on Mo/ZSM-5 catalysts to produce benzene and hydrogen: achievements and perspectives. Energy Environ Sci 1(5):526–541. https://doi.org/10.1039/B810981H

19. Matus EV, Sukhova OB, Ismagilov IZ, Tsikoza LT, Ismagilov ZR (2009) Peculiarities of dehydroaromatization of CH4-C2H6 and CH4 over Mo/ZSM-5 catalysts. React Kinet Catal Lett 98:59–67. https://doi.org/10.1007/s11144-009-0080-7
20. Holmen A (2009) Direct conversion of methane to fuels and chemicals. Catal Today 142(1):2–8. https://doi.org/10.1016/j.cattod.2009.01.004
21. Gambo Y, Jalil AA, Triwahyono S, Abdulrasheed AA (2018) Recent advances and future prospect in catalysts for oxidative coupling of methane to ethylene: a review. J Ind Eng Chem 59:218–229. https://doi.org/10.1016/j.jiec.2017.10.027
22. Cheng Z, Baser DS, Nadgouda SG, Qin L, Fan JA, Fan L-S (2018) C2 selectivity enhancement in chemical looping oxidative coupling of methane over a Mg–Mn composite oxygen carrier by li-doping-induced oxygen vacancies. ACS Energy Letters 3(7):1730–1736. https://doi.org/10.1021/acsenergylett.8b00851
23. Weckhuysen BM, Wang D, Rosynek MP, Lunsford JH (1998) Conversion of methane to benzene over transition metal ion zsm-5 zeolites: I. Catalytic characterization. J Catal 175(2):338–346. https://doi.org/10.1006/jcat.1998.2010
24. Abedin MA, Kanitkar S, Bhattar S, Spivey JJ (2020b) Methane dehydroaromatization using Mo supported on sulfated zirconia catalyst: effect of promoters. Catal Today. https://doi.org/10.1016/j.cattod.2020.06.071
25. Kosinov N, Coumans FJAG, Li G, Uslamin E, Mezari B, Wijpkema ASG, Pidko EA, Hensen EJM (2017) Stable Mo/HZSM-5 methane dehydroaromatization catalysts optimized for high-temperature calcination-regeneration. J Catal 346:125–133. https://doi.org/10.1016/j.jcat.2016.12.006
26. Tshabalala TE, Coville NJ, Anderson JA, Scurrell MS (2015) Dehydroaromatization of methane over Sn–Pt modified Mo/H-ZSM-5 zeolite catalysts: effect of preparation method. Appl Catal A 503:218–226. https://doi.org/10.1016/j.apcata.2015.06.035
27. Samanta A, Bai X, Robinson B, Chen H, Hu J (2017) Conversion of light alkane to value-added chemicals over ZSM-5/Metal promoted catalysts. Ind Eng Chem Res. https://doi.org/10.1021/acs.iecr.7b02095
28. Tshabalala TE, Coville NJ, Scurrell MS (2016) Methane dehydroaromatization over modified Mn/H-ZSM-5 zeolite catalysts: effect of tungsten as a secondary metal. Catal Commun 78:37–43. https://doi.org/10.1016/j.catcom.2016.02.005
29. Arata K (2009) Organic syntheses catalyzed by superacidic metal oxides: sulfated zirconia and related compounds. Green Chem 11(11):1719–1728. https://doi.org/10.1039/B822795K
30. Vosmerikova L, Barbashin Y, Vosmerikov A (2014) Catalytic aromatization of ethane on zinc-modified zeolites of various framework types. Pet Chem 54:420–425. https://doi.org/10.1134/S0965544114060103
31. Abedin MA, Kanitkar S, Kumar N, Wang Z, Ding K, Hutchings G, Spivey JJ (2020) Probing the surface acidity of supported aluminum bromide catalysts. Catalysts 10(8):869
32. Oloye FF, McCue AJ, Anderson JA (2016) n-Heptane hydroconversion over sulfated-zirconia-supported molybdenum carbide catalysts. Appl Petrochem Res 6(4):341–352. https://doi.org/10.1007/s13203-016-0172-z
33. Abedin MA, Kanitkar S, Bhattar S, Spivey JJ (2019) Promotional effect of Cr in sulfated zirconia-based mo catalyst for methane dehydroaromatization. Energy Technol 1900555
34. Rabee A, Mekhemer G, Osatiashtiani A, Isaacs M, Lee A, Wilson K, Zaki M (2017) Acidity-reactivity relationships in catalytic esterification over ammonium sulfate-derived sulfated zirconia. Catalysts 7(7):204
35. Abedin MA, Kanitkar S, Bhattar S, Spivey JJ (2020c) Sulfated hafnia as a support for Mo oxide: A novel catalyst for methane dehydroaromatization. Catal Today 343:8–17. https://doi.org/10.1016/j.cattod.2019.02.021
36. Reddy BM, Patil MK (2009) Organic syntheses and transformations catalyzed by sulfated zirconia. Chem Rev 109(6):2185–2208. https://doi.org/10.1021/cr900008m
37. Arata K (1990) Solid superacids. In: Eley DD, Pines H, Weisz PB (eds) Advances in catalysis, vol 37. Academic Press, Cambridge, pp 165–211. https://doi.org/10.1016/S0360-0564(08)60365-X
38. Parry EP (1963) An infrared study of pyridine adsorbed on acidic solids. Charact Surf Acidity. https://doi.org/10.1016/0021-9517(63)90102-7
39. Chen W-H, Ko H-H, Sakthivel A, Huang S-J, Liu S-H, Lo A-Y, Tsai T-C, Liu S-B (2006) A solid-state NMR, FT-IR and TPD study on acid properties of sulfated and metal-promoted zirconia: Influence of promoter and sulfation treatment. Catal Today 116(2):111–120. https://doi.org/10.1016/j.cattod.2006.01.025
40. Lay JJ, Li YY, Noike T (1998) The influence of pH and ammonia concentration on the methane production in high-solids digestion processes. Water Environ Res 70(5):1075–1082
41. Corma A (1997) Solid acid catalysts. Curr Opin Solid State Mater Sci 2(1):63–75. https://doi.org/10.1016/S1359-0286(97)80107-6
42. Levy RB, Boudart M (1973) Platinum-like behavior of tungsten carbide in surface catalysis. Science 181(4099):547–549
43. Bhattar S, Abedin MA, Shekhawat D, Haynes DJ, Spivey JJ (2020) The effect of La substitution by Sr- and Ca- in Ni substituted lanthanum zirconate pyrochlore catalysts for dry reforming of methane. Appl Catal A 602:117721. https://doi.org/10.1016/j.apcata.2020.117721
44. Querini CA (2004) Coke characterization. In: Spivey JJ, Roberts GW (eds) Catalysis, vol 17. The Royal Society of Chemistry, London, pp 166–209. https://doi.org/10.1039/9781847553294-00166
45. Liu W, Xu Y (1999) Methane dehydrogenation and aromatization over Mo/HZSM-5 In situ FT–IR characterization of its acidity and the interaction between Mo species and HZSM-5. J Catal 185(2):386–392. https://doi.org/10.1006/jcat.1999.2515
46. Lakhapatri SL, Abraham MA (2009) Deactivation due to sulfur poisoning and carbon deposition on Rh-Ni/Al2O3 catalyst during steam reforming of sulfur-doped n-hexadecane. Appl Catal A 364(1):113–121. https://doi.org/10.1016/j.apcata.2009.05.035
47. Katrib A, Logie V, Saurel N, Wehrer P, Hilaire L, Maire G (1997) Surface electronic structure and isomerization reactions of alkanes on some transition metal oxides. Surf Sci 377–379:754–758. https://doi.org/10.1016/S0039-6028(96)01488-4
48. Yun Y, Araujo JR, Melaet G, Baek J, Archanjo BS, Oh M, Alivisatos AP, Somorjai GA (2017) Activation of tungsten oxide for propane dehydrogenation and its high catalytic activity and selectivity. Catal Lett 147(3):622–632. https://doi.org/10.1007/s10562-016-1915-2
49. Hemming F, Wehrer P, Katrib A, Maire G (1997) Reactivity of hexanes (2MP, MCP and CH) on W, W2C and WC powders. Part II. Approach to the reaction mechanisms using concepts of organometallic chemistry. J Mol Catal Chem 124(1):39–56. https://doi.org/10.1016/S1381-1169(97)00069-1